The Role of Benzothiadiazole Unit in Organic Polymers on Photocatalytic Hydrogen Production

Martin Axelsson,[†] Ziyang Xia,[‡] Sicong Wang,[†] Ming Cheng,[*,‡] and Haining Tian[*,†]

[†]*Department of Chemistry Ångström, Uppsala University, Sweden*

[‡]*Institute for Energy Research, Jiangsu University, China*

E-mail: mingcheng@ujs.edu.cn; haining.tian@kemi.uu.se

Phone: +4618 471 3640

Abstract

Organic polymers based on the donor-acceptor structure are a promising class of efficient photocatalysts for solar fuel production. Among these polymers, poly(9,9-dioctylfluorene-alt-1,2,3-benzothiadiazole (PFBT) consisting of fluorene donor and benzothiadiazole acceptor units has shown good photocatalytic activity when it is prepared into polymer dots (Pdots) in water. In this work, we investigate the effect of the chemical environment on the activity of photocatalysis from PFBT Pdots for hydrogen production. This is carried out by comparing the samples with various concentrations of Palladium in different pH conditions and with different sacrificial electron donors (SDs). Moreover, a model compound 1,2,3 -benzothiadiazole di -9,9 -dioctylfluorene (BTDF) is synthesized to investigate the mechanism for protonation of benzothiadiazole and its kinetics in the presence of an organic acid – salicylic acid, by cyclic voltammetry. We experimentally show that benzothiadiazole in BTDF can rapidly react with protons with a fitted value of $0.1 - 5 * 10^{10} M^{-1} s^{-1}$ which should play a crucial role in the

photocatalytic reaction with polymer photocatalyst containing benzothiadiazole such as PFBT Pdots for hydrogen production in acidic conditions. This work gives insights into why organic polymers with benzothiadiazole work efficiently for photocatalytic hydrogen production.

Introduction

Filling the demands of being low-cost and tunable, with excellent light-absorbing properties organic polymers have risen as a type of promising photocatalysts for solar fuel production [1,2]. A common configuration of polymeric photocatalysts is based on so-called donor-acceptor structures with alternating electron-rich and electron-poor units to facilitate exciton formation from local excited states [3–5]. Since this type of polymer has been widely used in photodiodes as well as organic solar cells their photophysical and semi-conductive properties are widely studied [6–8]. As photocatalysts similarly the polymers have been mostly tuned to maximize their physical and optical properties, while studies of how and where the catalytic chemistry occurs are still few.

Many polymers and polymer nano-particles such as Pdots have shown that they have satisfactory photocatalytic hydrogen production even without the addition of a co-catalyst [9–12]. Since most of the polymers are synthesized by a coupling reaction in the presence of a Palladium(Pd)-catalyst [13,14], some Pd is typically trapped in the polymers and acts as co-catalysts. Kosco et al. have studied the effect of residual Pd remaining from synthesis on the performance of photocatalytic hydrogen evolution in (poly(9,9-dioctylfluorene-alt-1,2,3-benzothiadiazole) (F8BT or PFBT) and found that the photocatalytic activity has been completely inhibited when the polymer has less than 1 ppm Pd in the systems with 30%V of diethyl amine (DEA) as the sacrificial donor (SD) [15]. They also found that when the Pd content reached 40 ppm, the polymer could still produce a significant amount of hydrogen. However, the effect of the Pd co-catalyst seems to vary substantially from polymer to

polymer. Some polymers with a decent amount of Pd, show very low or absent activity for photocatalytic hydrogen production[11,12]. It implies that the polymer structure, especially the acceptor unit used in the polymer, should play an important role in the photocatalytic reaction even if the residual Pd is the catalytic site since the acceptor unit is where the electron is concentrated in an excited or reduced polymer.

Recently, Hillman et al. investigated the importance of sulfone units normally used in some polymers on photocatalytic hydrogen production and found that sulfone units play important roles in light absorption; hole transfer to triethylamine (TEA) SD, and electron transfer to residual Palladium[16]. Benzothiadiazole (BT) unit is also a common acceptor used in polymers that have shown good photocatalytic performance[11,17–19]. Recently, we have shown that a BT analogue benzothiadiazole dicarbonitrile (BTDN) could generate hydrogen on a glassy carbon electrode during the electrocatalytic conditions and the protonated intermediate species were studied[20]. The highest activity of photocatalytic hydrogen generation with polymers or Pdot photocatalysts involving BT units have been reported in acidic condition with ascorbic acid as the SD. Therefore, protonation of the BT unit probably is an important step for photocatalytic reaction. This motivated us to study the role of BT besides that of an electron acceptor during the photocatalytic reaction. PFBT polymer and a model compound (1,2,3 -benzothiadiazole di -9,9 -dioctylfluorene) (BTDF) as shown in Scheme 1 are therefore selected in this work.

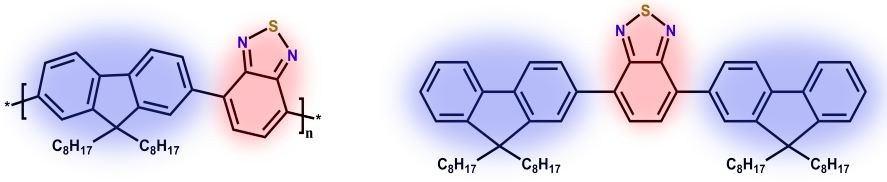

Scheme 1: The chemical structures of PFBT and BTDF.

Experimental Section

Materials

PFBT was purchased from Ossila. PFBT from the same batch was treated by Brilliant Matters to remove palladium until it was below the detection limit of 10 ppm. Polystyrene grafted with carboxy-terminated polyethylene oxide (PS-PEG-COOH, backbone chain Mw 8500 g mol^{-1}, graft chain Mw 4.6 kDa, total chain 36500 g mol^{-1}) was purchased from Polymer Source Inc. All solvents and other chemicals are purchased from Sigma-Aldrich and used as received unless stated otherwise.

Pdot Preparation

PFBT Pdots were prepared using the nano-precipitation method, where a 5:1 mixture of PFBT (40 μg mL^{-1}) and PS-PEG-COOH (8 μg mL^{-1}) was dissolved in THF. The THF phase was then quickly stirred into H_2O with a 1:2 ratio (V/V) while in an ultrasonication bath and then left in the bath for 10 minutes. Afterwards, the THF was left to evaporate in ambient conditions for two days. Pdots with different samples are compared by UV-Vis absorption spectroscopy (Figure S3) and dynamic light scattering (DLS) to get similar absorption intensity and particle size, respectively.

Photocatalytic Hydrogen Evolution

The photocatalytic hydrogen evolution experiments were performed in 9 mL gastight vials with 3 mL 20 µg mL^{-1} Pdots suspension. A 1.2 M ascorbic acid solution was prepared separately and modified to pH 4 with 3M NaOH. The Pdot suspension and ascorbic acid solution were degassed separately with argon gas, finally, 0.6 mL of the ascorbic acid was added to the Pdot suspension vial to a total of 3.6 mL. The vials were then illuminated

with a LED PAR38 lamp (17 W, 5000 K, Zenaro Lighting GmbH, $\lambda > 420$ nm) used as the light source, in a black box removing any stray light. The light intensity on the illuminated area of the vial is 50 mW cm^{-2}, which is measured and then calibrated with a power sensor (Thorlabs S120C, Si, 400 - 1100 nm, 50 mW connected to a PM100D console). The hydrogen was measured with a Gas chromatograph (PerkinElmer LLC, MA) calibrated from pure hydrogen injections. The H_2 was sampled by removing 100 µL gas from the headspace of the vial with a gas-tight Hamilton needle. Air was kept out of the vials by covering needle pinholes in the septum with Play-Doh clay (Hasbro, Inc) as the needles were retracted.

BTDF Synthesis

The synthetic route is shown in Scheme S1. 4,7-dibromo-2,1,3-benzothiadiazole (compound 1) (1.00 g, 3.40 mmol), 2-(9,9-dioctyl-9H-fluoren-2-yl)-4,4,5,5-tetramethyl-1,3,2-dioxaborolane (compound 2) (4.22 g, 8.16 mmol), $Pd(PPh_3)_4$ (0.12 g, 0.10 mmol), Aliquat 336 (0.069 g, 0.17 mmol), K_2CO_3 (3.76 g, 27.22 mmol), H_2O (30 mL), and toluene (90 mL) were placed in a round bottom flask. The reaction mixture was stirred at 110 °C under nitrogen for 24 h. After the reaction, the solution was cooled to room temperature, and it was then extracted with dichloromethane, the two phases were separated, and the water phase was extracted twice with dichloromethane. The combined organic extracts were washed three times with water, dried over Na_2SO_4, evaporated, and purified with column chromatography (eluding with petroleum ether/ dichloromethane, 5/1 v/v) to give 2.88 g of BTDF at a 92% yield. ^{1}H NMR (Chloroform-*d*, 400 MHz) δ 8.03 (dd, J = 7.9, 1.6 Hz, 2H), 7.96 (d, J = 1.6 Hz, 2H), 7.87 (d, J = 8.3 Hz, 4H), 7.80 – 7.73 (m, 2H), 7.41 – 7.31 (m, 6H), 2.04 (tq, J = 13.3, 5.4, 4.2 Hz, 8H), 1.21 – 1.05 (m, 40H), 0.80 (t, J = 6.9 Hz, 20H). ^{13}C NMR (Chloroform-*d*, 101 MHz) δ 14.09, 22.64, 23.94, 29.27, 29.75, 30.12, 31.85, 40.34 55.27, 119.74, 119.99, 122.99, 123.96, 126.88, 127.29, 127.90, 128.18, 133.64, 136.22, 140.71, 141.38, 151.13, 151.36, 154.42. HRMS-EIS (m/z): $[M + H]^+$ cacld for ($C_{64}H_{84}N_2S$), 913.4500, found: 913.6428. ^{13}C NMR ($CDCl_3$-*d*) δ 154.4, 151.4, 15.1.1, 141.4, 140.7, 136.2, 133.6, 128.2, 127.9, 127.3, 126.9, 124.0,

123.0, 120.2, 119.7, 55.3, 40.3, 31.8, 30.1, 29.8, 29.3, 23.9, 22.6, 14.1.

Cyclic Voltammetry

All cyclic voltammetry in organic solvents was performed in a ⊘ 2.5 x 5 cm cylindrical glass cell. The solvent used was THF (> 99.7% unstabilized (HPLC grade)) kept dry over 3Å molecular sieves, with 0.2 M recrystallized tetrabutylammonium hexafluorophosphate (TBA PF_6) as the supporting electrolyte. As working electrodes, either a ⊘ 3 mm glassy carbon disk or a ⊘ 3 mm Palladium disk electrodes were used and both were polished with a 0.05 μM Al particle paste in-between measurements, as a counter electrode a Pt wire was used. As a reference electrode, a silver-wire (Ag/Ag^+) pseudo reference was used in THF with the electrolyte in a glass tube connected to the solution with a porous vycore fritt, the potential is then confirmed with ferrocene as an internal standard. The water measurements were performed in a ⊘ 1.5 x 3 cm cylindrical cell with 50 mM KCl and 50 mM KH_2PO_4/K_2HPO_4 as electrolyte. The same working and counter electrodes were used as in the THF experiments but as a reference, a Ag/AgCl reference electrode was used. Highly concentrated samples (220 µg ml^{-1}) of Pdots were used in the aqueous conditions to enhance the signal. The 20 µg mL^{-1} Pdots sample was concentrated from 10 mL by centrifugal filtration with an Amicron Ultra-15 10k centrifugal filter at 5000 rpm for 12 minutes, leaving 0,9 mL Pdot solution.

Simulations

Electrochemical simulations were performed in DigiElch 8FD with the basic parameters $ks = 0.0012$ cm s^{-1} (rate constant for heterogeneous electron transfer), $\alpha = 0.5$ (the transfer coefficient), and $D_{BTDF} = 3.2 * 10^{-7}, D_{SAL} = 1.5 * 10^{-7}$ (the diffusion coefficients with all protonated intermediates set to D_{BTDF}) extracted from CVs of pristine BTDF in THF.

Results & Discussion

Condition dependency on H_2 evolution from Pdots

The photocatalytic proton reduction hydrogen evaluation of Pdots is considered a half-reaction of water splitting and the catalytic systems are normally optimized depending on SD used in the system. However, the SD used for the study also dictates what pH the system can operate in since the highest activity of the SD is dependent on the pH of the solution [21]. The pH of the catalytic system certainly has a significant effect on the catalytic performance since both the driving force to reduce protons and the catalytic mechanism can be affected by the presence of protons and the protic activity [22,23]. DEA and ascorbate are the two SDs that have been commonly used in the majority of the literature for photocatalysis with PFBT Pdots and therefore chosen in this study. DEA was reported at a basic condition, while ascorbate was reported at an acidic condition [10,11,15,24]. Therefore, we first compared the photocatalytic hydrogen production of PFBT Pdots with different residual Pd, at these two conditions.

The hypothesis is that if protonation of the BT unit is involved in the photocatalytic reaction, it would be more likely to occur in the acidic condition. At the same time, we also checked the effect of Pd amount in PFBT polymers on photocatalysis at different pH since the amount of active site should have a large impact on catalytic activity. Two PFBT samples with different Pd amounts, 1000 ppm, and less than 10 ppm Pd (below the detection limit), were chosen in this study. The Pdots from two PFBT samples were prepared as similarly as possible and then the photocatalytic experiments were carried out at two conditions: 0.2 M ascorbic acid with pH 4 [10,11,25,26] and 0.2 M DEA with pH of 13.5 (ca 11 vol% as compared to the 30 vol% used in the reference) [15,24]. Under these two reaction conditions, there is almost a ten orders of magnitude difference in proton concentration in the ascorbate condition (0.1 mM protons) as compared to that of the DEA condition (50

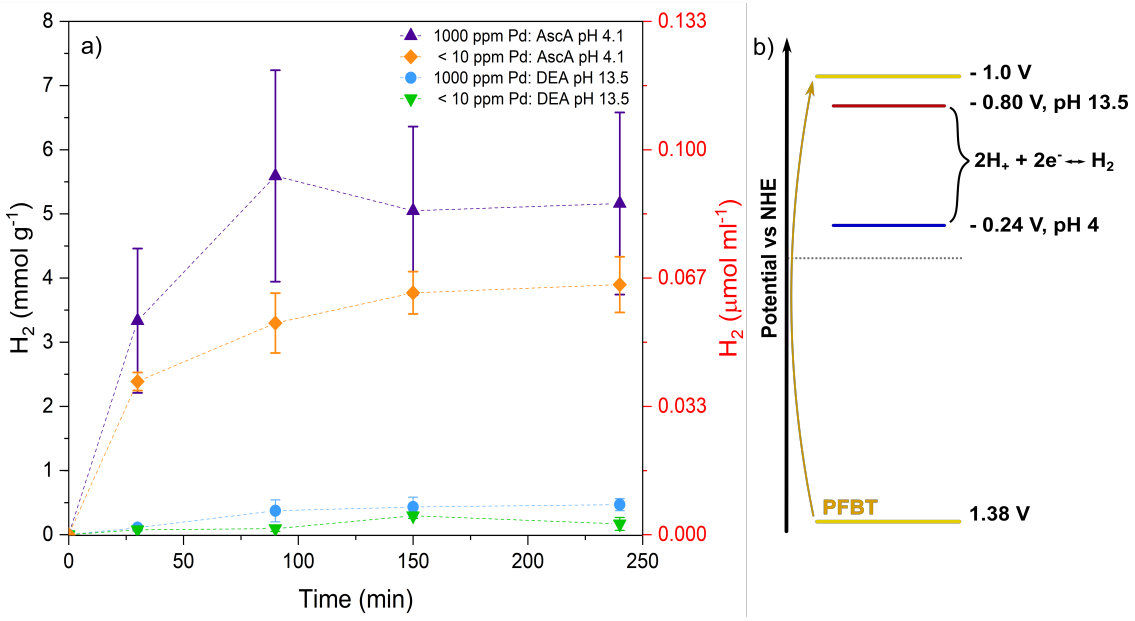

Figure 1: Comparison of different pH conditions and Pd content for photocatalytic hydrogen production. a) The photocatalytic hydrogen production under various conditions of hydrogen evolution from PFBT Pdots, ascorbate and high Pd content (purple triangles), ascorbate low Pd content (orange squares), DEA and high Pd content (blue circles), and DEA and low Pd content (green triangles). b) Scheme of the energy levels of PFBT and thermodynamic potentials for proton reduction at two different pH values.

fM protons). pH difference between 13.5 (DEA) and 4 (ascorbic acid) also leads to a large difference in driving force of 0.56 V for proton reduction.

As shown in Figure 1 b), at pH 13.5 in DEA, the driving force for PFBT polymer to reduce proton is only 0.2 V. The photocatalytic hydrogen evolution experiment (Figure 1 a)) shows a clear trend where the samples with acidic conditions significantly outperform the basic ones. None of the samples in the basic condition showed satisfactory hydrogen production (Figure S4). In acidic conditions, the sample with 1000 ppm Pd showed a slightly higher photocatalytic performance than that of the one with less than 10 ppm Pd. The large difference in driving force between the two pH conditions seems to be a major factor. Experiments with a systematical pH dependence for hydrogen production are useful to determine the change of photocatalytic activity of PFBT Pdots under various pH conditions. However, since SDs reductive activity is dependent on pH it is impossible to vary the pH

without affecting the availability of sacrificial electrons in the photocatalytic experiment. Instead, we, therefore, carried out electrocatalytic experiments under various pH conditions, to decouple the electron availability from the sacrificial donor and pH condition.

Electrocatalysis and pH dependence

We have previously demonstrated that PFBT Pdots could be active to generate hydrogen evolution on a glassy carbon electrode at acidic conditions[10]. Herein we performed the electrocatalysis of Pdots at various pH from 4-11.

The CVs (Figure 2) show a large catalytic current in acidic conditions that gets lower as the pH increases and then quickly drops off to zero between pH 7 and pH 8 (Figure S7). The current was confirmed to be from proton reduction by visible gas bubble formation at slower scan rates (Figure S8) and a hydrogen test from our previous work at pH 4[10]. The drop-off correlates well with the concentration of any acidic proton donor. At pH 4 and 6 the current looks to be dominated by free protons and the remaining current drops away at the pK_a value of dihydrogen phosphate at a pH of 7.2 where it is a higher concentration than the free H^+ ions. At higher pH values the protons would come from H_2O and the catalysis would have to swap from a water dissociation mechanism, which it seems unable to perform.

The experiments demonstrate that for reduced PFBT Pdots act as a catalyst, there needs to be a stronger proton donor than water in the system. The catalytic behaviour is also static in potential over the range of pH values that were tested and does not follow the reversible hydrogen electrode (RHE) (Figure S9). This behaviour indicates that the electrocatalysis relies on an initial reduction of the Pdots instead of a metal-based reaction, for example, a mechanism based on Pd metallic catalyst. The role of the BT unit, therefore, needs to be considered because it will be easier to protonate upon reduction in acidic conditions com-

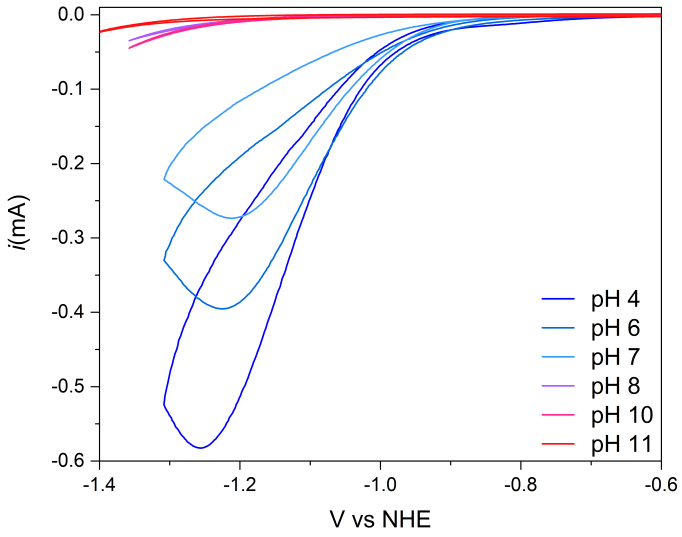

Figure 2: CVs demonstrating the pH dependence of electrocatalytic hydrogen evolution from PFBT Pdots, in 50 mM phosphate buffer and 50 mM KCl as the supporting electrolyte. Showing the decreasing catalytic current at 50 mVs^{-1} from pH 4 to pH 7 with a collapse of current between pH 7 and pH 8.

pared to basic conditions. If the protonation of BT is faster than the electron transfer to residual Pd from reduced PFBT, the protonation of BT is therefore a possible intermediate involved in the photocatalytic reaction. To compare how Pd-centered catalysis looks in the system a Pd working electrode with the same area as the GC electrode (⊘ 3 mm), the Pd-based mechanism does radically differ from what is seen with the GC electrode (Figure S10).

In our previous work, we could monitor the protonation of the BT analogue BTDN, from CV in presence of an organic acid, salicylic acid[20]. We therefore first looked into the CV of pristine PFBT polymer both for the washed and the commercial as-received polymer while dissolved in THF. The electrochemical behaviour of PFBT is very complex with many available redox states (Figure S11). It is however clear that the reduced polymer reacts with acids in a solution (Figure 3 a)) by a positive shift of the wave which is characteristic of a reaction following a reduction. To elucidate what kind of reaction is and calculate the rate

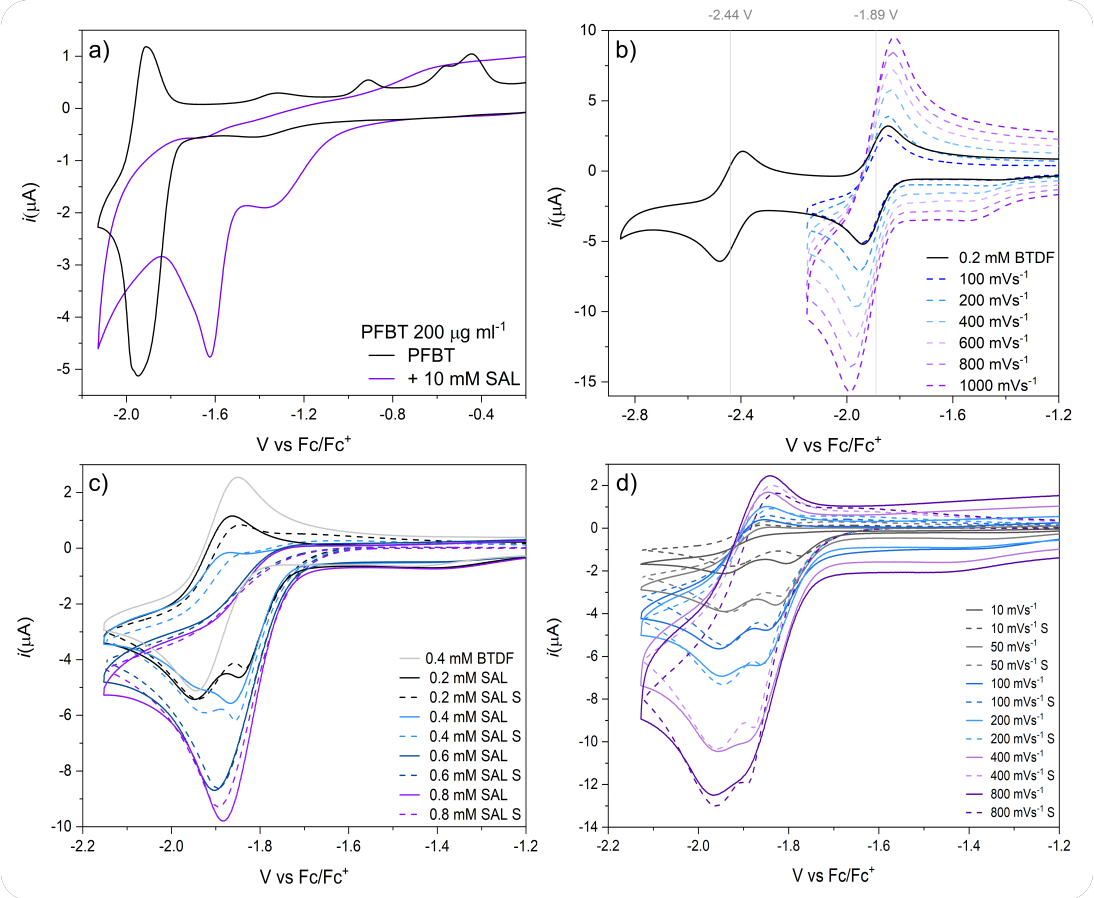

Figure 3: Cyclic voltammograms of BTDF and PFBT recorded in THF. a) CVs of the pristine PFBT polymer in THF at 200 µg mL^{-1} with and without the addition of a proton donor (salicylic acid) recorded at 100 mVs^{-1}. b) CVs of 0.2 mM BTDF with the $E_{1/2}$ values and with varied scan rates with the current having a linear dependence on the square root of the scan rate. c) A titration of 0.4 mM BTDF with salicylic acid (0.2-0.8 mM) and the corresponding simulated CVs (dashed lines). d) CVs of 0.4 mM BTDF with 0.4 mM SAL with varying scan rate (10-800 mVs^{-1}) and the corresponding simulated CVs (dashed lines).

of the protonation step, we designed and synthesized a model compound BTDF consisting of one BT unit and two fluorene units to mimic the PFBT polymer and use for more in-depth electrochemistry studies.

Electrochemical properties of BTDF

BTDF shows a similar electronic structure to the PFBT polymer with the BT excitation and fluorene-related transition around 320 nm as well as a band from their interaction around 420 nm, both of these transitions are retained in the polymer but red-shifted due to the increased electron delocalization in the large conjugated system of the PFBT polymer[20,27–29] (Figure S12). In comparison to the PFBT polymer, the redox behaviour of BTDF is very clear with two reversible reductions at 1.89 and -2.49 V vs Fc/Fc^{+}, and a linear scan rate dependence of the square root of the current as would be expected of a freely diffusing molecule. The two reversible reductions of BTDF are similar to that of the molecule BTDN (600 mV in between reductions as compared to 800 mV in BTDN) , however, shifted to more negative potentials due to the difference in electron richness between the side groups. The electron-donating dioctylfluorene units make the BT unit more difficult to be reduced as compared to the electron-withdrawing nitrile groups in BTDN[20].

When adding salicylic acid as a proton donor to a BTDF solution in THF, there was a clear shift to the CV where the reduction becomes irreversible with a shift to more positive potentials and with an increase in current. In the conditions of the acids at the first reduction potential, BTDF did not perform catalysis for proton reduction (Figure S13). This can be explained by the high reductive potential that is probably required to reduce BTDF further which is the requirement for the proton reduction by BTDN on a glassy carbon electrode[20]. However, with glassy carbon under this condition, there is not an electrochemical window to reduce BTDF further. The clean voltammetric behaviour of BTDF at its first reduction potential is good enough for us to investigate the protonation mechanism of the BT unit of BTDF in detail.

The protonation mechanism of BT unit can be extracted from the behaviour of the shift in the first reduction wave. At high concentrations (more than two equivalents) of acid, the

wave is completely irreversible with a doubling in electric current. Including the positive shift, this is the mark of two consecutive follow-up reactions, a so-called EC (electrochemical step followed by a chemical step) reaction that is followed by a secondary reduction step either another electrode-based electron transfer (an ECE reaction: an EC reaction followed by a secondary electrochemical step) or an intermolecular charge transfer between the newly generated species similar to what happens in BTDN (a so-called EC-DISP reaction: an EC reaction followed by a disproportionate reaction)[30]. To disentangle the two types of reactions, an acid titration and a scan rate dependence experiment were performed (Figure 3 c) and d)). During the titration, it can be seen that the reduction peak splits into two different peaks at lower acid concentrations and then merge at higher concentrations. At higher scan rates a merge of the two peaks can be seen as well as a slight return of the oxidation peak showing that the irreversible nature of the reaction is dependent on the scan rate. The two data sets were then used to simulate the protonation mechanism.

Fitting a mechanism to the CV data (Figure3) c), d)) shows that the overall BTDF reduction reaction follows an ECEC type reaction (an ECE reaction followed by a second chemical step) where the second reduction step occurs at a less reductive potential than the first reduction, -0.5 V compared to -1.89 V vs Fc/Fc^+ in this case, but any value on closer to zero than -1 V vs Fc/Fc^+ fits the data quite well (Scheme 2). A key feature to getting the peak-splitting and then merging at higher acid concentrations is that the first protonation is an equilibrium that is heavily shifted towards the protonated species with reaction kinetics around or exceeding the diffusion limit at 0.1-5 $*10^{10} M^{-1} s^{-1}$ but the back reaction ($2 *10^{7} M^{-1} s^{-1}$) is still faster than the next protonation step $2 *10^{6} M^{-1} s^{-1}$.

The result shows that the BT unit does react with protons at least once when reduced. As the chemical environment of BT in BTDF and PFBT is highly similar, we believe this protonation should happen in PFBT polymers as well when it is reduced.

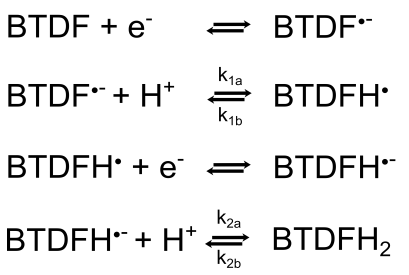

E_0 (V vs Fc/Fc^+)	k_a (s^{-1} M^{-1})	k_b (s^{-1} M^{-1})
- 1.89	—	—
—	$5*10^9$	$2*10^7$
- 0.50	—	—
—	$2*10^6$	10

Scheme 2: The simulated mechanism (left) and kinetic constant (right) of the reaction between reduced BTDF and protons.

Exciton Quenching of Pdots by an Electron Acceptor

While the electrochemical studies show that the reduced PFBT polymer will react with sufficiently strong acids, the photochemical case does not have to be so straightforward. In the photochemical system, there is not a large pool of high-energy electrons to reduce the polymer instead the generated exciton will have to be reductively quenched by the SD to get the reduced polymer. However, the exciton can, in theory, dissociate in many different ways, not only reductively, in PFBT both reductive quenching from DEA and oxidative quenching Pd particles have been previously reported[24].

But the electron transfer from excited PFBT to Pd clusters via oxidative quenching has been reported as a main charge separation process for photocatalysis with PFBT in the presence of DEA[24].

Oxidative quenching of PFBT by residual Pd has been reported up to at least 50% with 1170 ppm Pd while still quenching around 25% with as low as 36 ppm Pd. However, the reductive quenching of PFBT by SDs to form reduced PFBT also seems to be an important pathway with 20-30% quenching in 30% DEA and 40% in Ascorbic acid[10,24]. We can also see a clear reductive quenching of PFBT in organic media with ascorbic acid (Figure S14-15), since this is a condition with sufficiently acidic protons that the reduced polymer is expected

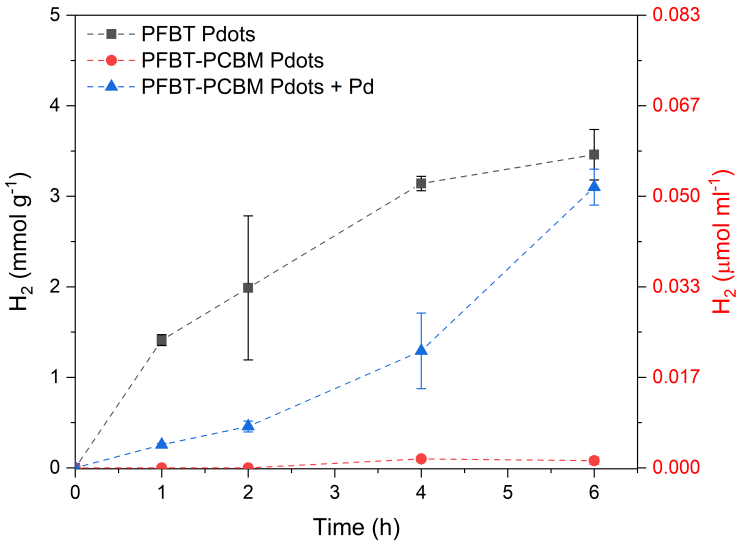

Figure 4: The photocatalytic hydrogen data for three different compositions of PFBT Pdots in pH 4 with ascorbic acid as the SD: unmodified PFBT Pdots (grey squares), PFBT-PCBM binary Pdots (red circles), and photo-deposited Pd in PFBT-PCBM binary Pdots (blue triangles).

to rapidly be protonated. This is even more likely with ascorbic acid as it will also release a proton as it decomposes after being oxidized and therefore works like a proton-coupled electron transfer (PCET) donor and not just a simple reductive agent[31–33].

Therefore, it is also likely that electron transfer to an active Pd site could also happen from an already protonated reduced polymer. In this case, it is possible that the proton would transfer as well, as it has already been shown that BT sites will perform proton-coupled electron transfer reactions[20]. This certainly requires that the residual Pd is close enough to the active site. It however generates a question: what is the form of residual Pd in the PFBT polymer?

It is hard to get direct spectral evidence from NMR or IR due to the low ppm level concentrations, except the transient spectroscopic data[24]. Instead, we used phenyl-C61-butyric acid methyl ester (PCBM) to extra electrons from PFBT in a binary PFBT: PCBM Pdots.

If the residual Pd is a cluster acting as the catalytic site, then the reduced PCBM generated after electron transfer from PFBT under light illumination should still be able to give electrons to the Pd cluster for catalysis as well, similarly as Pd clusters can get electrons from the PFBT polymer. However, the photocatalysis was completely inhibited in presence of PCBM, unless an extra Pd or Pt source is introduced afterwards (Figure 4, S16). This cannot be well explained by the unreachable Pd cluster by PCBM due to a well-embedded Pd cluster in PFBT. Moreover, we should still be able to observe hydrogen production anyway, because the Pd cluster could still get electrons after competing with PCBM from reduced or excited PFBT for catalysis due to fast electron transfer between PFBT to Pd (fs-ns)[24].

Therefore, we hypothesize that the catalytically active residual Pd site has a favourable interaction for electron transfer with the BT unit. Perhaps, reduced PFBT with protonated BT units at acidic conditions even works as both electron proton channels to the active species. If the residual Pd is the only catalytic site in PFBT polymer, then the catalytically active Pd sites should be much less than the Pd amount detected by ICP, it is also evident from the comparable photocatalytic performance from the samples with 1000 ppm and less than 10 ppm Pd.

Conclusions

In summary, we have studied the effect of chemical environments on the photocatalysis of PFBT Pdots and concluded that the protonation of benzothiadiazole (BT) in PFBT polymer could be an important intermediate process for photocatalysis in acidic conditions. From photocatalytic experiments, the PFBT sample with less than 10 ppm Pd showed comparable photocatalytic activity to the sample with 1000 ppm. It indicates that the active residual Pd amount should be much less than the actual residual Pd in the polymer if Pd is the only

catalytic site. With a model compound BTDF in electrochemical experiments, the reaction rate of protonation of BT unit is found to be a fast and diffusion-controlled reaction. The results suggest that the protonated BT likely is an important intermediate of PFBT polymer at acidic conditions, indicating a possible proton-coupled electron transfer (PCET) process from the reduced protonated polymer to the intrinsic catalytic sites. This work, therefore, paves the road to understanding the reaction mechanism of polymeric photocatalysts with heteroatom block units.

Acknowledgement

H.T. gratefully thanks Swedish Research Council (grant no. 2017-03757, 2021-03859) for the financial support. M. C. acknowledges the financial support from the National Natural Science Foundation of China (Grants 22179053, 22279046), Natural Science Excellent Youth Foundation of Jiangsu Provincial (BK20220112). The authors also give their great appreciation to Pierre-Olivier Morin from Brilliant Matters for the help with purifying PFBT polymer to lower the amount of residual Pd.

Supporting Information Available

Experimental procedures, characterization of products, spectroscopic and voltammetric data, and control experiments.

The following files are available free of charge.

- Filename: SIBenzothiadiazoleUnitinOrganicPolymers.pdf

References

(1) Pavliuk, M. V.; Wrede, S.; Liu, A.; Brnovic, A.; Wang, S.; Axelsson, M.; Tian, H. Preparation, characterization, evaluation and mechanistic study of organic polymer

nano-photocatalysts for solar fuel production. *Chemical Society Reviews* **2022**, *51*, 6909–6935.

(2) Wang, Y.; Vogel, A.; Sachs, M.; Sprick, R. S.; Wilbraham, L.; Moniz, J. A. S.; Godin, R.; Zwijnenburg, M. A.; Durrant, J. R.; Cooper, A. I.; Tang, J. Current understanding and challenges of solar-driven hydrogen generation using polymeric photocatalysts. *Nature Energy* **2019**, *4*, 746–760.

(3) Havinga, E.; Hoeve, W. t.; Wynberg, H. A new class of small band gap organic polymer conductors. *Polymer Bulletin* **1992**, *29*, 119–126.

(4) Havinga, E.; Hoeve, W. t.; Wynberg, H. Alternate donor-acceptor small-band-gap semiconducting polymers; Polysquaraines and polycroconaines. *Synthetic Metals* **1993**, *55*, 299–306.

(5) Gibson, G. L.; McCormick, T. M.; Seferos, D. S. Atomistic Band Gap Engineering in Donor–Acceptor Polymers. *Journal of the American Chemical Society* **2012**, *134*, 539–547, PMID: 22129273.

(6) Zhan, X.; Zhu, D. Conjugated polymers for high-efficiency organic photovoltaics. *Polym. Chem.* **2010**, *1*, 409–419.

(7) Sekine, C.; Tsubata, Y.; Yamada, T.; Kitano, M.; Doi, S. Recent progress of high performance polymer OLED and OPV materials for organic printed electronics. *Science and Technology of Advanced Materials* **2014**, *15*, 034203.

(8) Zhang, G.; Lin, F. R.; Qi, F.; Heumüller, T.; Distler, A.; Egelhaaf, H.-J.; Li, N.; Chow, P. C. Y.; Brabec, C. J.; Jen, A. K.-Y.; Yip, H.-L. Renewed Prospects for Organic Photovoltaics. *Chemical Reviews* **2022**, *122*, 14180–14274.

(9) Sprick, R. S.; Jiang, J.-X.; Bonillo, B.; Ren, S.; Ratvijitvech, T.; Guiglion, P.; Zwijnenburg, M. A.; Adams, D. J.; Cooper, A. I. Tunable Organic Photocatalysts for

Visible-Light-Driven Hydrogen Evolution. *Journal of the American Chemical Society* **2015**, *137*, 3265–3270.

(10) Wang, L.; Fernández-Terán, R.; Zhang, L.; Fernandes, D. L. A.; Tian, L.; Chen, H.; Tian, H. Organic Polymer Dots as Photocatalysts for Visible Light-Driven Hydrogen Generation. *Angewandte Chemie - International Edition* **2016**, *55*, 12306–12310.

(11) Pati, P. B.; Damas, G.; Tian, L.; Fernandes, D. L. A.; Zhang, L.; Pehlivan, I. B.; Edvinsson, T.; Araujo, C. M.; Tian, H. An experimental and theoretical study of an efficient polymer nano-photocatalyst for hydrogen evolution. *Energy and Environmental Science* **2017**, *10*, 1372–1376.

(12) Bai, Y.; Wilbraham, L.; Slater, B. J.; Zwijnenburg, M. A.; Sprick, R. S.; Cooper, A. I. Accelerated Discovery of Organic Polymer Photocatalysts for Hydrogen Evolution from Water through the Integration of Experiment and Theory. *Journal of the American Chemical Society* **2019**, *141*, 9063–9071.

(13) Miyaura, N.; Yamada, K.; Suzuki, A. A NEW STEREOSPECIFIC CROSS-COUPLING BY THE PALLADIUM-CATALYZED REACTION OF 1-ALKENYLBORANES WITH 1-ALKENYL OR l-ALKYNYL HALIDES. *Tetrahedron Letters* **1974**, *20*, 3437–3440.

(14) Miyaura, N.; Suzuki, A. Palladium-Catalyzed Cross-Coupling Reactions of Organoboron Compounds. *Chemical Reviews* **1995**, *95*, 2457–2483.

(15) Kosco, J.; Sachs, M.; Godin, R.; Kirkus, M.; Francas, L.; Bidwell, M.; Qureshi, M.; Anjum, D.; Durrant, J. R.; McCulloch, I. The Effect of Residual Palladium Catalyst Contamination on the Photocatalytic Hydrogen Evolution Activity of Conjugated Polymers. *Advanced Energy Materials* **2018**, *1802181*, 1802181.

(16) Hillman, S. A. J.; Sprick, R. S.; Pearce, D.; Woods, D. J.; Sit, W.-Y.; Shi, X.; Cooper, A. I.; Durrant, J. R.; Nelson, J. Why Do Sulfone-Containing Polymer Photo-

catalysts Work So Well for Sacrificial Hydrogen Evolution from Water? *Journal of the American Chemical Society* **2022**, *144*, 19382–19395.

(17) Yang, C.; Ma, B. C.; Zhang, L.; Lin, S.; Ghasimi, S.; Landfester, K.; Zhang, K. A. I.; Wang, X. Molecular Engineering of Conjugated Polybenzothiadiazoles for Enhanced Hydrogen Production by Photosynthesis. *Angewandte Chemie* **2016**, *128*, 9348–9352.

(18) Huang, W.; He, Q.; Hu, Y.; Li, Y. Molecular Heterostructures of Covalent Triazine Frameworks for Enhanced Photocatalytic Hydrogen Production. *Angewandte Chemie International Edition* **2019**, *58*, 8676–8680.

(19) Xu, Y.; Mao, N.; Zhang, C.; Wang, X.; Zeng, J.; Chen, Y.; Wang, F.; Jiang, J.-X. Rational design of donor-π-acceptor conjugated microporous polymers for photocatalytic hydrogen production. *Applied Catalysis B: Environmental* **2018**, *228*, 1–9.

(20) Axelsson, M.; Marchiori, C. F.; Huang, P.; Araujo, C. M.; Tian, H. Small Organic Molecule Based on Benzothiadiazole for Electrocatalytic Hydrogen Production. *Journal of the American Chemical Society* **2021**, *143*, 21229–21233.

(21) Pellegrin, Y.; Odobel, F. Les donneurs d'électron sacrificiels pour la production de combustible solaire. *Comptes Rendus Chimie* **2017**, *20*, 283–295.

(22) Villalba, M.; Peron, J.; Giraud, M.; Tard, C. pH-dependence on HER electrocatalytic activity of iron sulfide pyrite nanoparticles. *Electrochemistry Communications* **2018**, *91*, 10–14.

(23) Lasia, A. Mechanism and kinetics of the hydrogen evolution reaction. *International Journal of Hydrogen Energy* **2019**, *44*, 19484–19518.

(24) Sachs, M.; Cha, H.; Kosco, J.; Aitchison, C. M.; Francàs, L.; Corby, S.; Chiang, C.-L.; Wilson, A. A.; Godin, R.; Fahey-Williams, A.; Cooper, A. I.; Sprick, R. S.; McCulloch, I.; Durrant, J. R. Tracking Charge Transfer to Residual Metal Clusters in

Conjugated Polymers for Photocatalytic Hydrogen Evolution. *Journal of the American Chemical Society* **2020**, *142*, 14574–14587.

(25) Hu, Z.; Wang, Z.; Zhang, X.; Tang, H.; Liu, X.; Huang, F.; Cao, Y. Conjugated Polymers with Oligoethylene Glycol Side Chains for Improved Photocatalytic Hydrogen Evolution. *iScience* **2019**, *13*, 33–42.

(26) Yang, H.; Li, X.; Sprick, R. S.; Cooper, A. I. Conjugated polymer donor–molecular acceptor nanohybrids for photocatalytic hydrogen evolution. *Chem. Commun.* **2020**, *56*, 6790–6793.

(27) Griffiths, J. *Colour and constitution of organic molecules*; Academic Press, 1976.

(28) Rogers, J. E.; Nguyen, K. A.; Hufnagle, D. C.; McLean, D. G.; Su, W.; Gossett, K. M.; Burke, A. R.; Vinogradov, S. A.; Pachter, R.; Fleitz, P. A. Observation and Interpretation of Annulated Porphyrins Studies on the Photophysical Properties of meso-Tetraphenylmetalloporphyrins. *The Journal of Physical Chemistry A* **2003**, *107*, 11331–11339.

(29) Hanson, K.; Roskop, L.; Djurovich, P. I.; Zahariev, F.; Gordon, M. S.; Thompson, M. E. A Paradigm for Blue- or Red-Shifted Absorption of Small Molecules Depending on the Site of π-Extension. *Journal of the American Chemical Society* **2010**, *132*, 16247–16255.

(30) Savéant, J.; Costentin, C. *Elements of Molecular and Biomolecular Electrochemistry*; 2019.

(31) Creutz, C. The Complexities of Ascorbate as a Reducing Agent. *Inorganic Chemistry* **1981**, *20*, 4449–4453.

(32) Williams, N.; Yandell, J. Outer-sphere electron-transfer reactions of ascorbate anions. *Australian Journal of Chemistry* **1982**, *35*, 1133–1144.

(33) Warren, J. J.; Tronic, T. A.; Mayer, J. M. Thermochemistry of Proton-Coupled Electron Transfer Reagents and its Implications. *Chemical Reviews* **2010**, *110*, 6961–7001.